

Anand constitutive model of lead-free solder joints in 3D IC device

Liang Zhang^{1,2}, Zhi-quan Liu², Yu-tong Ji³

¹ School of Mechanical and Electrical Engineering, Jiangsu Normal University, Xuzhou 221116, China

² Institute of Metal Research, Chinese Academy of Sciences, Shenyang 110016, China

³ School of Information and Art, Jiangsu Vocational Institute of Architectural Technology, Xuzhou 221116, China

Email: zhangliang@jsnu.edu.cn

Abstract. Anand constitutive relation of SnAgCu and SnAgCu-nano Al solders were studied under uniaxial tension, and the constitutive model was used in the finite element simulation to analyze the stress-strain response of lead-free solder joints in 3D IC devices. The results showed that the nine parameters of the Anand model can be determined from separated constitutive relations and experimental results. Based on Anand model, the finite element method was selected to calculate the stress-strain response of lead-free solder joints, it was found that in the 3D IC device the maximum stress-strain concentrated in the concern solder joints, the stress-strain of SnAgCu-nano Al solder joints was lower than that of SnAgCu solder joints, which represented that the addition of nano Al particles can enhance the reliability of lead-free solder joints in 3D IC devices.

1. Introduction

Since the implementation of the Restriction of Hazardous Substances (RoHS) directives nearly a decade ago, there have been new developments and several improvements in lead-free solders to replace the conventional SnPb solders for using in the electronics industry^[1,2]. Among serial lead-free solders investigated, SnAg/SnAgCu base solders with excellent properties were proposed as the most promising substitute^[3,4]. However, the low creep resistance^[5] and brittle bulk IMC^[6] maybe two important drawback of these solder in service for high-density devices.

For 3D IC structure, three-dimensional (3D) stacking of integrated circuits (ICs) possesses unique advantages, which include the enhancement of device density per volume, utilization of short vertical interconnection for improved electrical performance, and the capability of integrating multiple functions into a single package^[7]. In Ni/SnAg/Ni 3D IC application, it is found that the optimal weight percentage of Ag is between 2.4 and 3.5 wt.% to inhibit the formation of microvoids^[8]. Moreover, the Sn, SnAgCu also were reported as interconnection materials in 3D IC, which can determine the reliability of electronic devices in service. Due to large difference in the coefficient of thermal expansion (CTE)^[9] of the different constituents in the 3D assembly, thermal stress were created in solder joints during thermal process. Therefore, the reliability of solder joints in 3D IC should be studied further in service.

In this paper, SnAgCu and SnAgCu bearing 0.1% Al nanoparticles were selected to be used in 3D IC, the Anand constitutive model of these solders was obtained by tensile tests, and the model was



incorporated into finite element simulation to analyze the stress-strain response of solder joints in service, which can be utilized to evaluate the reliability of 3D IC device.

2. Anand model

2.1. Experimental procedure

SnAgCu solders bearing Al nano-particles were prepared via mechanically incorporating 0.1% of about 20-25nm Al nanoparticles into Sn3.8Ag0.7Cu solder paste for about 15 minutes to promote uniform particle distribution. Then the paste with no-clean flux was printed on Cu substrates, then the samples were heated in an industrial reflow oven, the molten alloys were chill cast ingots in a ceramics mold. Then they were solidified by nominally air-cooling. All solder specimens were heat treated at 125°C for an hour to stabilize the microstructure of the SnAgCu and SnAgCu-nanoAl solder alloys. The dog-shaped bulk solder specimens for the uniaxial tensile test were prepared, by machining from extruded SnAgCu and SnAgCu-nanoAl solder bar. The solder specimens have a total length of 65mm, a gage length of 15mm, and a diameter of 3mm.

A series of uniaxial tensile tests of the SnAgCu and SnAgCu-nanoAl solders were performed with a number of different strain rates and temperature conditions. The tests were conducted at tensile strain rates ranging from $1.0 \times 10^{-4} \text{ s}^{-1}$ to $1.0 \times 10^{-2} \text{ s}^{-1}$, and at temperatures of -55°C, -25 °C, 25 °C, 75 °C, and 125 °C. True strain control mode was employed and true strain rate was maintained constant during the tests until specimen failure occurred.

2.2. Anand equations

Anand and Brown have established the constitutive equations for large, isotropic, viscoplastic deformations but small elastic deformations, and the equation is the single-scalar internal variable model [10,11]. Within the frame work of this model, there appears a scalar valued function for the equivalent plastic strain rate and an evolution equation for the internal variable [12]. Anand model incorporates viscoplastic, time-dependent plastic phenomenon where the development of plastic strain is dependent on the rate of loading, viscoplasticity is defined by unifying plastic and creep deformations [13]. In this constitutive model, two basic features can be found obviously [14,15]. Firstly, this model need no explicit yield condition and no loading/unloading criterion, the plastic strain is assumed to take place at all nonzero stress values, although at low stresses the rate of plastic flow may be immeasurably small; secondly, this model employs a single scalar as an internal variable to represent the isotropic resistance to plastic flow offered by the internal state of the material, the single scalar variable s represents an averaged isotropic resistance to macroscopic plastic flow offered by the underlying isotropic strengthening mechanisms.

The internal variable s in the model characterizes isotropic hardening mechanism such as dislocation density, solid solution hardening, and subgrain and grain size effects, etc., and the relationship between deformation resistance and the equivalent stress can be represented as [16],

$$\sigma = cs \quad (1)$$

where c is a function of strain rate and temperature as expressed in the following equation, s is the deformation resistance with the dimensions of stress, σ is the equivalent stress for the steady plastic flow. Moreover, c is defined as follows:

$$c = \frac{1}{\dot{\epsilon}} \sinh^{-1} \left[\left(\frac{\sigma}{A} \exp(Q/RT) \right)^m \right]$$

(2)

With the combination of equations (1) and (2), the flow equation of the Anand model was constructed to exactly accommodate the strain rate dependence on the stress at constant structure [17]:

$$\dot{\epsilon} = A \exp\left(-\frac{Q}{RT}\right) \left[\sinh\left(\xi \frac{\sigma_0}{s}\right) \right]^{1/m} \quad (3)$$

where $\dot{\epsilon}$ is the inelastic strain rate, A is pre-exponential factor, Q is the activation energy, R is universal gas constant, T is the temperature, ξ stands for the materials constant, m is the strain rate sensitivity.

Moreover, the evolution equation for the internal variable s is assumed to be the form as

$$\dot{s} = h(\sigma_0, T) \dot{\epsilon} \quad (4)$$

where

$$h = h_0 \left| 1 - \frac{s}{s^*} \right|^a \text{sign}\left(1 - \frac{s}{s^*}\right) \quad a \geq 1 \quad (5)$$

Therefore, the evolution equation for the internal variable s is derived with the combination of equations (4) and (5) as

$$\dot{s} = \left\{ h_0 \left| 1 - \frac{s}{s^*} \right|^a \text{sign}\left(1 - \frac{s}{s^*}\right) \right\} \dot{\epsilon} \quad (6)$$

where

$$s^* = \left\{ \frac{\dot{\epsilon}}{A} \exp(Q/RT) \right\}^n \quad (7)$$

where h_0 represents the hardening/softening constant, n stands for the strain rate sensitivity for the saturation value of deformation resistance, a is the strain rate sensitivity of hardening/softening, s^* describes the saturation value of s associated with a set of given temperature and strain rate, and ξ is a coefficient.

Anand model includes two kinds of equations, the first equation deals with the relationship between saturation stress and strain rate under certain temperature, while the second equation deals with relationship between strain and stress under certain strain rate and temperature^[18]. From equations (1), (2) and (7), together with $\sigma^* = c s^*$, the equations are as follows:

$$\sigma^* = \frac{\sigma_0}{\xi} \left[\frac{\dot{\epsilon}}{A} \exp(Q/RT) \right]^n \sinh^{-1} \left[\left(\frac{\dot{\epsilon}}{A} \exp(Q/RT) \right)^m \right] \quad (8)$$

Equation (8) includes the saturation stress, temperature and strain rate.

From equations (1) and (6), with isothermal, and $s^* > s$ conditions, we can obtain:

$$\frac{d\sigma}{d\dot{\epsilon}} = c h_0 \left| 1 - \frac{\sigma}{\sigma^*} \right|^a \text{sign}\left(1 - \frac{\sigma}{\sigma^*}\right), \quad a \geq 1 \quad (9)$$

To estimate the remaining parameters, all of the stress-strain data from the monotonic tests is used to fit the following stress-strain relationship^[19]:

$$\sigma = \sigma_0 - \left[(\sigma_0 - \sigma_0)^{(1-a)} + (a-1) \left\{ (c h_0) (\sigma_0)^{-a} \right\} \dot{\epsilon} \right]^{1/(1-a)}, \quad a \neq 1 \quad (10)$$

where $\sigma_0 = c s_0$ and s_0 is the initial value of s .

2.3. Parameters analysis

For the Anand constitutive model, nine parameters need to be tested respectively. These materials constants A , Q/R , $\dot{\epsilon}$, h_0 , ξ , m , n , a and s_0 can be determined by the following standard procedures^[20]:

- (1) Obtained the saturation stresses from uniaxial tensile tests with constant rates and temperatures.
- (2) Determined the value of A , Q , $\dot{\epsilon}/\xi$, h_0 , ξ , m and n in equation (8) from the data acquired in step (1) by a non-linear least square fit. The nonlinear least squares fit to the experimental data was obtained using the Levenburg-Marquardt Algorithm which was coupled to a driver subroutine that exercised the constitutive model and generated uniaxial tension for any prescribed set of material parameters.
- (3) Determined $\dot{\epsilon}$ and ξ from the values obtained in step(2). The parameter ξ was selected that the constant c in equation(2) was less than unity, and $\dot{\epsilon}$ was then determined from the combined term $\dot{\epsilon}/\xi$.
- (4) The combined constants $c h_0$, $c s_0$ and a in equation(10) were determined from the constant strain rate data by a least square fit. With the value of c gotten in step(3), h_0 and s_0 were conclude.

The materials parameters of Anand model for the SnAgCu and SnAgCu-nanoAl lead-free solders determined by this procedure are listed in Table 1.

Table 1 Material parameters of Anand model for lead free solders

Solder	A/s^{-1}	$Q/R/K^{-1}$	$\dot{\epsilon}/MPa$	h_0/MPa	ξ	m	n	a	s_0/MPa
SnAgCu-nanoAl	22100	8015	59	4132	4.1	0.15	0.0154	2.0	27
SnAgCu	24300	8710	62.3	3541.2	5.8	0.183	0.019	1.9	39.5

3. Finite element simulation

The quarter model of 3D IC structure was established because of the geometric symmetry of the assembly, which can reduce the computational procedure. The SOLID45 linear element is used for meshing all the materials except solder joints, the VISCO107 linear element (8-nodes element), which describes the viscoplastic material behavior, is utilized to mesh solder joints in finite element software. The model of 3D IC structure under consideration consists of lead-free solder joints (SnAgCu-nanoAl and SnAgCu), Cu pillars and two Chips, which is shown in Fig. 1. And selective mesh refinement is used to concentrate highly refined element in the solder joints where is most likely to fail, sparse elements for other materials. Moreover, zero displacement constraints of vertical direction of the cross-area were applied to the cross-sections of the 1/4 model, namely all nodes on the symmetric surface ($X=0$, $Z=0$) were fixed in the corresponding directions (X , Z), and the node at the origin ($X=Y=Z=0$) was fixed in any directions.

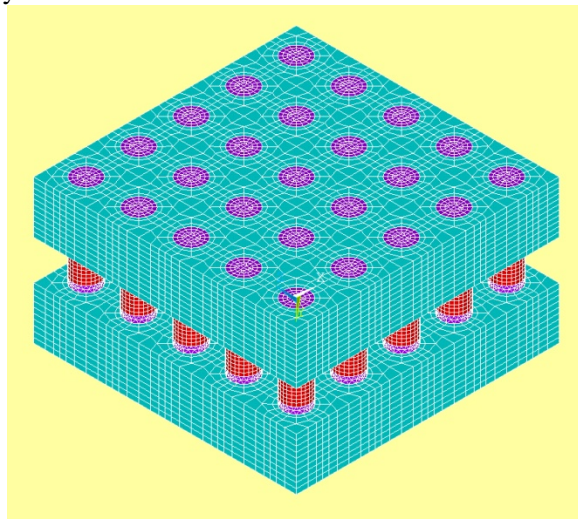


Fig.1 Quarter model of 3D IC structure

In the finite element simulation, accelerated thermal cycling loading (218K-398K) was selected to evaluate the reliability of lead-free solder joints in 3D IC, and the thermal cyclic loading was selected to be imposed on the 3D IC structure. The temperatures ranging from 218K to 398K was carried out for the testing, and the reference temperature (initial temperature) is 298K, dwell time at all peak temperature is 15min, the rates of descend and ascend temperature are 12 K/min. Moreover, it is assumed that in the finite element simulation no stress occurs at the initial temperature. For the thermal cycle loading, at all nodes in the 3D IC structure were loaded a uniform temperature distribution.

Because the thermal mismatch among the chips, Cu, solder joints is linearly dependent on the DNP (distance to neutral point), the highest von Mises stress can be found in the corner solder joints. Fig.2 show the von Mises stress distribution of the solder joints in the array, it is demonstrated that the von Mises stress increases obviously with the increase of DNP, the corner solder joint is the critical solder joints, and the largest von Mises stress was observed on the corner solder joint near the chip.

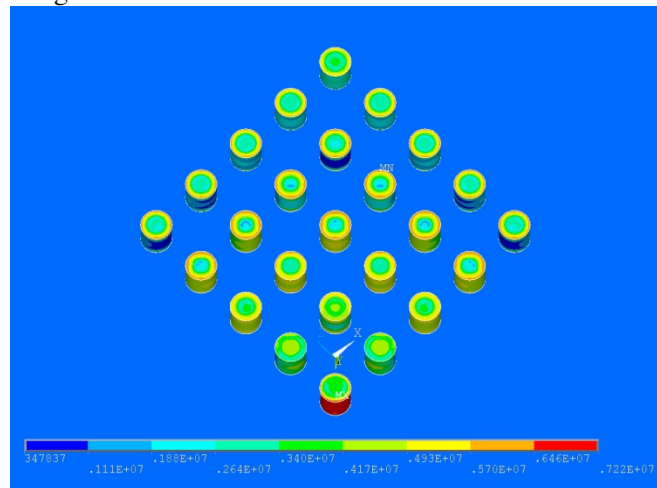


Fig.2 Von Mises stress distribution of solder joints

Due to the CTE (coefficient of thermal expansion) of the materials in the 3D IC, the stress-strain can be happened in the solder joints, so with the finite element simulation results, the fatigue life of SnAgCu/ SnAgCu-nanoAl solder joints in 3D IC structure can be calculated. The modified Coffin–Manson equation is still the most convenient tool for estimating the thermal fatigue life of solder joint. Engelmaier developed the model and utilized to solder joints fatigue prediction, the Engelmaier modified fatigue equation can be written as

$$N_f = \frac{1}{2} \left(\frac{\Delta\gamma}{2\varepsilon'_f} \right)^{1/c} \quad (11)$$

where N_f is the fatigue life, $\Delta\gamma$ is the inelastic shear strain range per cycle calculated using finite element simulation, ε'_f is the fatigue ductility coefficient which is taken as $2\varepsilon'_f = 0.514$, c is the fatigue ductility exponent which is approximately -0.5708 for SnAgCu based solder joints. It should be noted that, in the present study, the modified Coffin–Manson equation is applied using the data from finite element elements with the inelastic highest shear strain.

Table 2 Fatigue lives of SnAgCu-nanoAl and SnAgCu solder joints

Solder joints	Inelastic shear strain	Fatigue life
SnAgCu-nanoAl	0.0065	1057.34
SnAgCu	0.0052	1563.12

Table 2 shows the fatigue life of SnAgCu and SnAgCu-nanoAl solder joints calculated using the modified Coffin–Manson equation based on finite element simulation. The fatigue life of SnAgCu-nanoAl solder joints is higher than that of SnAgCu solder joints, reflecting the increase of the fatigue resistance in the solder joint to some extent, the addition of nano-Al particles can increase the fatigue life by 47.8% compared with the SnAgCu solder joints during thermal cycling loading. The phenomena can be attributed to the reduction of the fatigue damages and the change of microcrack propagation sites during the fracture process, which depends on the refinement of intermetallic compounds due to the Al nanoparticles addition^[21].

4. Conclusions

The Anand model of SnAgCu and SnAgCu-nano Al solders were studied under uniaxial tension, the model was incorporated into finite element simulation in 3D IC structure. It was found that in the 3D IC device the maximum stress-strain concentrated in the concern solder joints, the stress-strain of SnAgCu-nano Al solder joints was lower than that of SnAgCu solder joints, the fatigue life which represented that the addition of nano Al particles can enhance the reliability of lead-free solder joints in 3D IC devices.

Acknowledge

This study was funded by the Natural Science Foundation of China(51475220), the Qing Lan Project, the China Postdoctoral Science Foundation funded project(2016M591464) and the State Foundation of Laboratory of Advanced Brazing Filler Metals & Technology (Zhengzhou Research Institute of Mechanical Engineering) (SKLABFMT-2015-03).

References

- [1] Kanlayasiri K, Sukpimai K. 2016. Journal of Alloys and Compounds, **668**, 169.
- [2] Zhang L, Tu K N. 2014. Materials Science & Engineering: R: Reports, **82**,1.
- [3] Ji F, X S B, Zhang L, Gao L L, Sheng Z, Dai W. 2011. Chinese Journal of Mechanical Engineering, **24**,428.
- [4] Sun L, Zhang L, Zhong S J, Ma J, Bao L. 2015. Journal of Materials Science: Materials in Electronics, **26**, 9164.
- [5] Zhang L, Fan X Y, Guo Y H, He C W. 2014. Electronic Materials Letters, **10**,645.
- [6] Yang L, Zhang Y C, Dai J, Jing Y F, Ge J G, Zhang N. 2015. Materials and Design, **67**,209.
- [7] Shen Y L, Johnson R W. 2013. Microelectronics Reliability, **53**,79.
- [8] Yu J J, Yang C A, Lin Y F, Hsueh C H, Kao C R. 2015. Journal of Alloys and Compounds, **629**,16..
- [9] Amalua E H, Ekerea N N, Zarmaia M T, Takyib G. 2015. Finite Elements in Analysis and Design, **107**,13.
- [10] Anand L. 1985. International Journal of Plasticity, **1**,213.
- [11] Brown S B, Kim K H, Anand L. 1989. International Journal of Plasticity, **5**, 95.
- [12] Wu R, McCluskey F P. 2008. Thermal and Thermomechanical Phenomena in Electronic Systems, Orlando, FL, May, 683-686.
- [13] Ye H, Lin M H, Bassaran C. 2002. Finite Elements in Analysis and Design, **38**, 601.
- [14] Hu X D, Ju D Y. 2006. Transactions of Nonferrous Metals Society of China, **16**, 586.
- [15] Chen X F, Liang L H, Liu Y, Wang Q. 2009. Chinese Journal of Applied Mechanics, **26**,248.
- [16] Chen X, Chen G, Sakane M. 2004. The Ninth Intersociety Conference on Thermal and Thermomechanical Phenomena in Electronic Systems, June1-4, 447.
- [17] Cheng Z N, Wang G Z, Chen L, Wilde J, Becker K. 2000. Soldering & Surface Mount Technology, **12**, 31.
- [18] Pang J H L, Low P T H, Xiong B S. 2004. The Ninth Intersociety Conference on Thermal and Thermomechanical Phenomena in Electronic Systems, June1-4, 131.
- [19] Bahate D, Chan G, Subbarayan G. 2008. IEEE Transactions on Components and Packaging

- Technologies, **31**, 622.
- [20] Bai N, Chen X, Gao H. 2009. Materials and Design, **30**,122.
- [21] Zhang L, Han J g, Guo Y h, Sun L. 2015. Journal of Materials Science: Materials in Electronics, **26**, 3615.